Novel L-Slot Matching Circuit Integrated with Circularly Polarized Rectenna for Wireless Energy Harvesting

Mohamed M. Mansour [1,2,*] and **Haruichi Kanaya** [1]

[1] Graduate School of Information Science and Electrical Engineering, Kyushu University, Fukuoka 819-0395, Japan; kanaya@ed.kyushu-u.ac.jp
[2] Microelectronics Department, Electronics Research Institute, Giza 12622, Egypt
* Correspondence: m.mansour01@ieee.org or mansour.mohamed.485@s.kyushu-u.ac.jp; Tel.: +81-92-802-3746

check for updates

Abstract: Radio frequency (RF) power harvesting allows wireless power delivery concurrently to several remote RF devices. This manuscript presents the implementation of a compact, reliable, effective, and flexible energy harvesting (EH) rectenna design. It integrates a simple rectifier circuit with a circularly polarized one-sided slot dipole antenna at 2.45 GHz Industrial, Scientific, Medical (ISM) frequency band for wireless charging operation at low incident power densities, from 1 to 95 $\mu W/cm^2$. The rectenna structure is printed on a single layer, low cost, commercial FR4 substrate. The integration of the rectifier and antenna produces a low-profile and high performance circularly polarized rectenna. In order to maximize the system efficiency, the matching circuit introduced between the rectifier and antenna is optimized for a minimum number of discrete components and it is constructed using multiple of L-slot defects in the ground plane. For a given input power of -6 dBm intercepted by the circularly polarized antenna with 3 dBi gain, the peak RF-DC (radio frequency-direct current) conversion efficiency is 59.5%. The rectenna dimensions are 41×35.5 mm^2. It is demonstrated that the output power from the proposed rectenna is higher than the other published designs with a similar antenna size under the same ambient condition. Thanks to its compact size, the proposed rectenna finds a range of potential applications for wireless energy charging.

Keywords: circular-polarized; energy harvesting; rectenna; rectifier; wireless charging

1. Introduction

The development of wireless communications is largely promoted by the desire of freely communicating anywhere and anytime. However, due to the constraint of electrical wires, continuous power supply is affected, which also limits the freedom of communication. If electric power can be supplied wirelessly, not only can great freedom be brought to the communication industry, but also a reliable guarantee can be provided for charging the wireless sensor network nodes. Engineers are frequently challenged to realize energy-efficient end-applications, but those challenges multiply when trying to design for ultra-low power Internet of Things (IoT) applications [1,2]. The IoT is an emerging key technology for future industries and everyday people life, where an infinite number of battery operated sensors, actuators, and smart objects are connected to the internet to provide services such as mobile healthcare, intelligent transport system, environmental monitoring, etc. Since energy efficiency is of utmost importance to these battery constrained IoT devices, IoT-related standards and research works have focused on the device energy conserving issues. The conventional method for powering these sensors was obsolete and new technologies were developed to provide power

smoothly to the remote sensor units. The RF energy harvesting technique offers a substantial solution for battery replacement and maintenance. It could re-charge the battery wirelessly using a radiated electromagnetic energy either available in the environment or primarily generated from a huge RF transmitter. Consequently, these applications are expected to communicate with other systems and operate autonomously for years.

Several operating frequencies of the rectenna have been considered and investigated in literature [3–8]. Design of microwave power transmission has traditionally been focused on 2.45 GHz where it has the following advantages: comparably low atmospheric loss, cheap components, and the highest reported conversion efficiency [9]. On the other side, a self-powered sensor node is composed of antenna, rectifier, and in some cases a power management unit. The rectifier can be constructed using several diode topologies, for example, single-series diode, single-shunt diode or a diode bridge [10]. Among those topologies, the single-diode configuration that serves as half-wave rectification is the simplest and preferred design for an efficient rectifier design at low-power levels [11,12]. Single-diode topology offers a simple and low-cost construction, which requires very few components. The available amount of ambient RF power is varying from location to another. Several studies investigated the available RF power densities in various regions in the world [13,14].

The remainder of the manuscript is organized into several sections. Literature survey and the related work to the current study is presented in Section 2. Then, the proposed system, the rectifier circuit layout and its extracted circuit model, and the antenna design procedure are discussed in Section 3. Section 4 is devoted to the rectenna integration and the measurement setup. The results and a detailed discussion are introduced in Section 5. Conclusions are drawn in Section 6.

2. Related Work

Recently, several studies focus on the optimum design of the antenna was proposed. Its objective is to maximize the input power thus improving the overall RF-DC conversion efficiency. In order to increase the RF-DC conversion efficiency, authors have suggested to utilize either, antenna array, wideband frequency harvesting or high Q factor components at a specific operating frequency. The most preferred antenna architecture is the one that exhibits a circular polarization feature. A circularly polarized rectenna doesn't require strict alignment between transmitting and receiving antennas. In literature, many circular polarized antenna structures have been developed [15,16].

In [17], a compact double-layer rectenna was introduced and it is based on a tapered annular slot and a single-diode rectifier. A dual circularly polarized patch antenna in which a high-order harmonic rejection property is embedded and a pair of rectifying circuits without harmonic rejection filters have been proposed in [18]. Despite the high efficiency introduced by that design (82.3% at 22 dBm), the resulting devices are large and more difficult to install.

The rectenna architecture is decomposed of two main components, the radiating element, and the rectifying circuit as shown in Figure 1. The radiating element is an antenna with effective aperture area (A_{eff}) which converts electromagnetic waves with a power density (S_{RF}) into an electrical signal guided into a cable to the subsequent stages. The rectifying circuit is constructed using Schottky diode and it is responsible for transforming alternate current (AC) electrical energy into DC voltage. The LPF improves the DC smoothness at the terminal load resistance R_L.
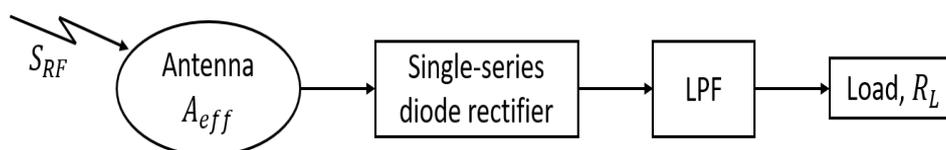
Figure 1. Block diagram of the wireless energy harvesting system. A plane wave received by the antenna element has power density S_{RF}. Subsequent stages are the rectifier circuit, low-pass filter (LPF), and the load that consumes the DC power.

In this scenario, a compact and high efficient CP rectenna is proposed. The novelty of the design lies on the simplicity to implement a high-efficient energy harvesting rectenna using a single layer metal constructed on a low-cost commercial FR4 substrate. The proposed topology not only offers a new method to design the rectifier circuit as it avoids the use of surface mount devices (SMD) for realizing the matching circuit, but it also employs simple rectifier topology comprised of single diode-capacitor connection. Furthermore, the rectenna size of the previous proposed work is quite large and the circuit structure is also very complex. Thus, such rectennas are not suitable for some indoor miniaturized small sensors.

3. Proposed System

This article reports an efficient rectifier operating at 2.45 GHz for wireless energy harvesting applications with low input power levels. In order to minimize the number of discrete components and hence the conduction losses, a single series diode topology is adapted for operation with low input power level. Indeed, the coplanar waveguide (CPW) configuration is selected for the rectifier and antenna configuration. This topology is chosen due to the high-frequency performance and ease of implementation. It also reduces the coupling effect and allows for easy inclusion of series and shunt elements. The analytical approach is discussed to evaluate the rectifier performance in conjunction with the effect of the matching circuit. The equivalent circuit model is predicted and compared with both the experimental and the EM model. A structurally flexible and simple CP slot antenna has been proposed. With controlling the length of the open stub introduced inside the antenna slot, the proposed antenna can provide a tuned impedance matching at different frequency bands. In this design, the 3 dB AR bandwidth can reach as large as 200 MHz (2.4–2.6 GHz) which is about 8.2% (relative to the center frequency of 2.45 GHz) to cover the Wi-Fi band 2.4–2.5 GHz (IEEE 802.11 standards). The proposed design also has a voltage standing wave ratio, VSWR < 2, an impedance bandwidth of 600 MHz (2.3–2.9 GHz), which is approximately 25% relative to the center frequency of 2.45 GHz. The rectifier circuit is integrated with the antenna on the same substrate. The entire experimental performance of the rectenna is characterized and compared to the simulation results. In this section, the theory and analysis of the antenna and rectifier topology is discussed. The rectifier is simply composed of a single-series diode configuration and the matching circuit is extensively presented in Section 3.1. The antenna has a one-sided slot dipole CPW structure and a circularly-polarized feature; more details are introduced in Section 3.2.

3.1. RF Rectifier Design

The key components of a rectifier are the diode(s), a low-pass filter and a resistive load. The diode is the most considerable components because it should convert the limited available RF power into exploitable DC energy. A good rectifier must have low power consumption, good power sensitivity, and good power handling capability [19]. The diode chosen for the present application is a Schottky diode SMS7630-061F [20]. It is selected because of its low turn-on voltage and small junction capacitance, which enables it to work at the desired high frequencies.

The choice of a rectifier topology design is critical for efficient power harvesting. A single matched low-power diode in the series configuration is selected for the rectifier topology because it uses few lumped components, has a reduced size, and introduces low losses and ease of fabrication. The selected topology is shown in Figure 2.

The rectifier topology is based on a very simple and attractive CPW configuration given in Figure 3a, and the proposed circuit topology employs only single Schottky diode and a capacitor that behaves as LPF for smoothing the DC voltage at the rectifier output. Therefore, the design is very interesting in the aspect of deploying few lumped elements.

The impedance matching circuit is crucial for maximum power transfer between the antenna and the rectifier input. Implementation of the matching circuit is not simple since the rectifier is a nonlinear load with a complex impedance that varies with frequency, input power level and the

built-in characteristics of the diode. In order to obtain the optimum diode performance, the rectifier circuit is optimized in conjunction with the matching circuit.
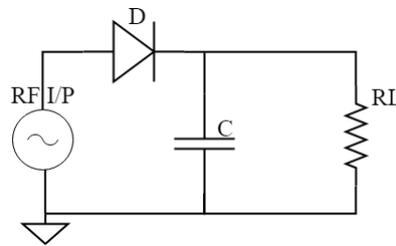
Figure 2. Block diagram of the wireless energy harvesting system.
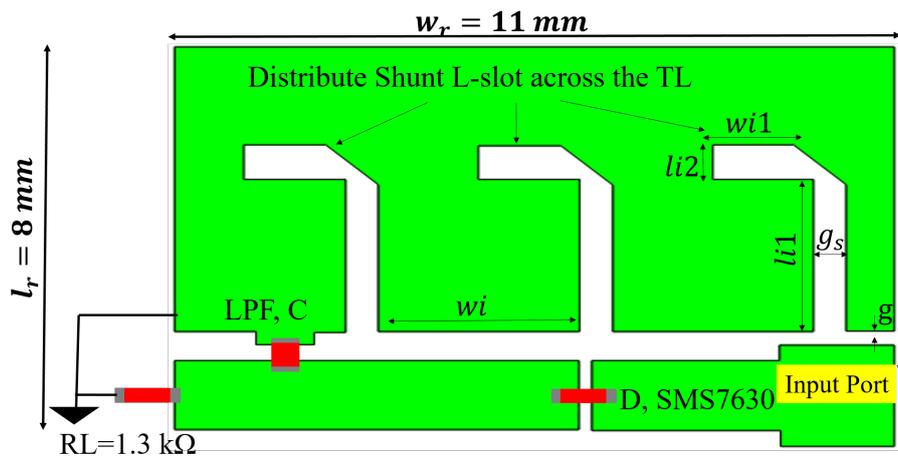
(a)
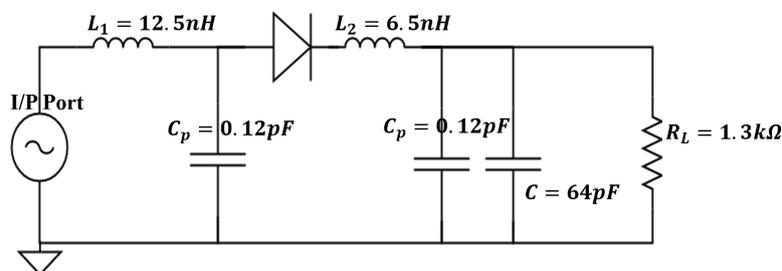
(b)

Figure 3. The RF rectifier circuit (**a**) rectifier layout and the dimensions are as follows: $w_{i1} = 1.7$ mm, $l_{i1} = 3.14$ mm, $l_{i2} = 0.74$ mm, $w_i = 3.25$ mm, $g_s = 0.53$ mm, $g = 0.3$ mm; (**b**) equivalent circuit model.

The matching circuit is simply formed by inserting defects in the ground plane. The defects are multiple of L-slots distributed along the transmission line. Single L-slot is $\lambda_g/10$ short-ended transmission line at the frequency of interest. To ensure the optimum DC power output, the number of slots was optimized using the ADS software. The effect of cascading the number of slots on the rectifier input characteristics will be investigated later.

The rectifier circuit is analyzed using the circuit model approach and the electromagnetic (EM) approach. The analytical circuit model derived from the rectifier layout is shown in Figure 3b. To illustrate, each slot has inductance L(nH); this inductance is derived from the input impedance (Z_{in}) of a shorted lossless transmission line that has characteristic impedance Z_o and propagation constant β. The inductance estimated using the well-known equations [21] is $L = 6.5$ nH. The first two slots comprises a series pair of inductance so they can be estimated as $2 \times L$. In order to consider the coupling inside the slot gap, a shunt capacitor is introduced between the main transmission line and

the ground. After full optimization of such components, the circuit model parameters are given by ($L_1 = 12.5$ nH, $L_2 = 6.5$ nH and $C_p = 0.12$ pF).

The simulations were carried out in the ADS software and the typical comparison between EM-model simulation, circuit model and measurements are shown in Figure 4a. The curves demonstrate the results agreement between EM and the extracted circuit model along with the operating band. To show the rectifier design flexibility, a cascading number of slots were considered and simulated using both EM and circuit model. The number of slots can significantly change the resonance frequency as shown from the EM and circuit simulation in Figure 4b. The circuit model of each case was derived based on the previous discussion. The optimum number of slots selected for the current design is three, as they produce a good matching along with the desired frequency band.

(a)   (b)
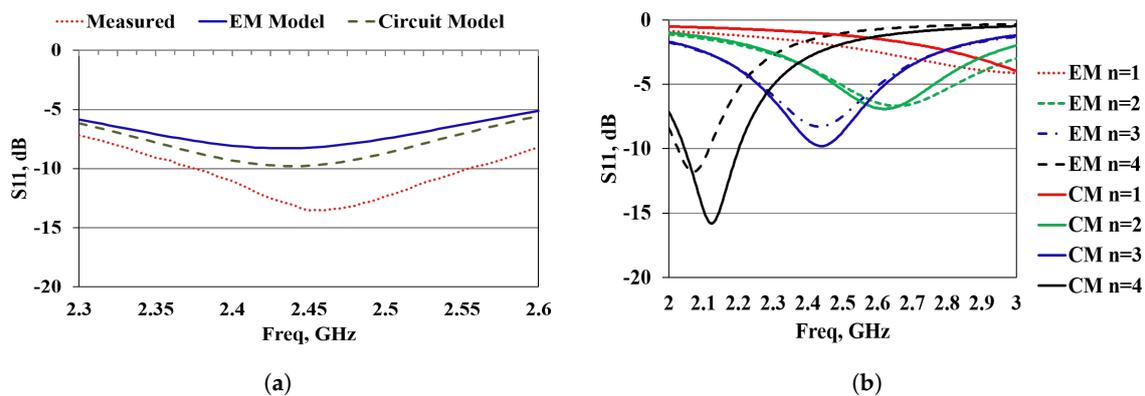
Figure 4. The simulation characteristics of the RF rectifier circuit, (a) return loss S_{11}; (b) effect of cascading L-slot along the transmission line (EM: stands for EM model simulation, CM: circuit model simulation, and *n* represents the number of slots).

3.2. Antenna Design Architecture

Both the rectifier and antenna structure are constructed using CPW configuration by removing the ground on either side of the signal strip line [22]. Some of the advantages of CPW arise from the fact that the mounting of lumped (active or passive) components in shunt or series configuration is much easier, drilling of holes through the substrate is not needed, and transition to slotline is less cumbersome, thereby allowing greater flexibility in the use of mixed transmission media.

The slot antenna (shown in Figure 5a) consists of a radiator formed by cutting a narrow slot in a large metal surface given by $l \times w$, where l is the length and w is the width of the antenna. The slot is formed by L-section slot with a length of approximately in the order of half wavelength at the desired frequency and the width is optimized (using HFSS simulation software V.13 Ansys Co.) for proper impedance matching as given in Figure 5b. The surface current distribution on the antenna geometry is shown in Figure 5c for different input phase excitation. From the plots, the current is rotated counterclockwise. Consequently, it shows a left-handed circular polarization (LHCP). The antenna is printed onto FR4 substrate using CPW transmission line configuration. It is fed by a 50 Ω-CPW feeding line, where the signal strip and the gap have 2.16 mm and 0.3 mm, respectively.

The radiation and matching characteristics of the antenna are illustrated in Figure 6. The antenna return loss (S_{11}) across the operating band is shown in Figure 6a. It is noted that both measured and simulated results are well matched across the operating band with more than -10 dB around the center frequency 2.45 GHz. The proposed design also has VSWR < 2 with matching impedance bandwidth 600 MHz (2.3–2.9 GHz), which is approximately 25% relative to the center frequency of 2.45 GHz. To prove the CP of the proposed antenna, the axial ratio AR is plotted in Figure 6b. The measured 3 dB AR bandwidth can reach as large as 100 MHz (2.4–2.5 GHz), which is about 4% (relative to the center frequency of 2.45 GHz) to cover the Wi-Fi band 2.4–2.5 GHz (IEEE 802.11 standards), which meets the prior design specifications. The antenna gain is explained in Figure 6c.

As shown, the maximum realized gain (3 dBi) is slightly shifted from the resonance frequency. This is attributed to the tolerance during the measurement setup.

(a)

(b)

(c)
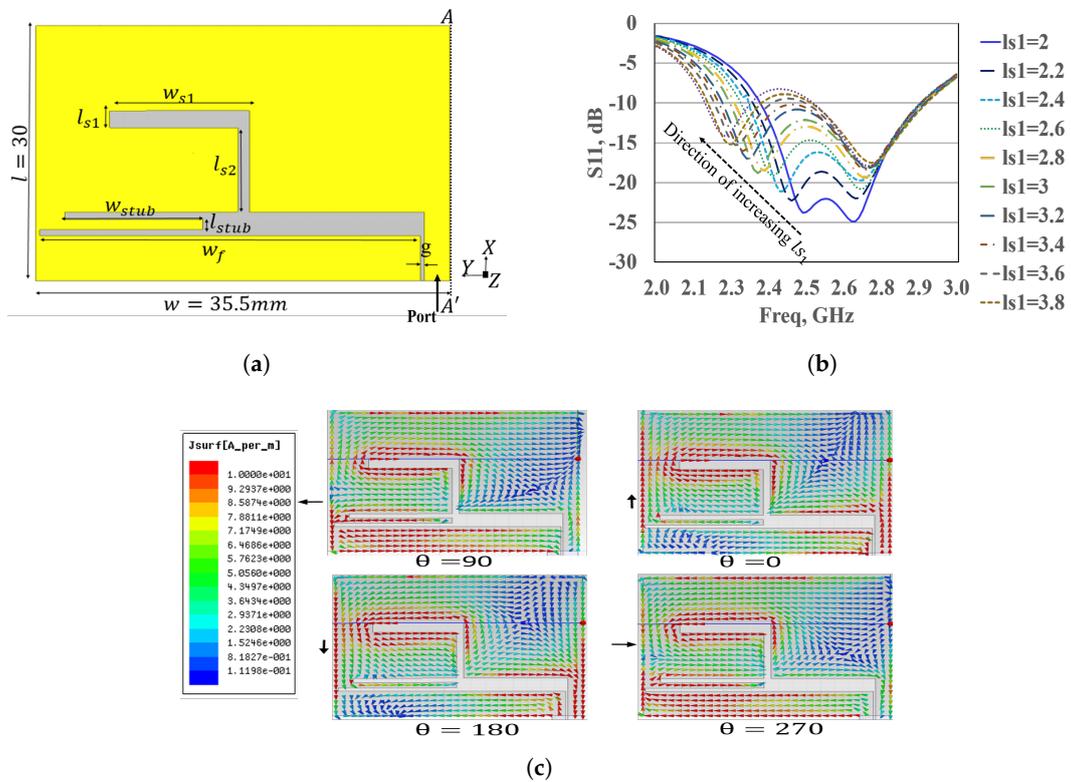
Figure 5. The antenna configuration and parametric study. (**a**) The CPW antenna layout, the dimensions are as follows: $w_{s1} = 12$ mm, $l_{s1} = 2$ mm, $l_{s2} = 9.9$ mm, $w_{stub} = 11.84$ mm, $l_{stub} = 1.2$ mm, $w_f = 32.7$ mm, $g = 0.3$ mm; (**b**) the effect of changing the L-slot width l_{s1}; (**c**) surface current distribution on the antenna structure for different phase excitation at frequency 2.45 GHz.

(a)

(b)

(c)
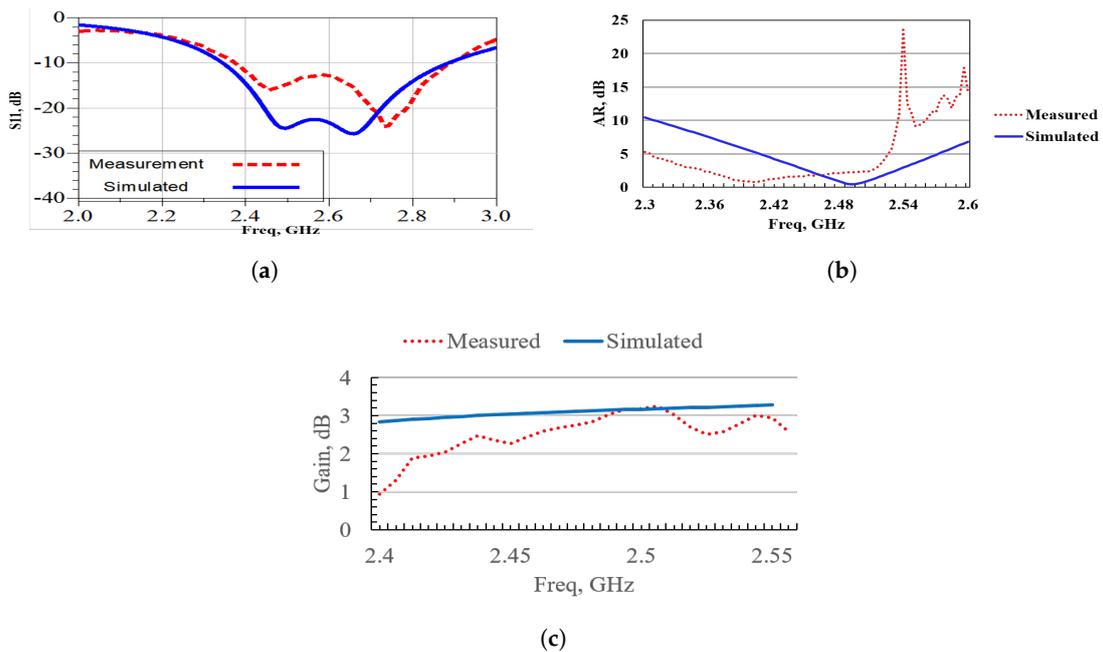
Figure 6. The measurement and simulation characteristics of the slot antenna (**a**) return loss S_{11}; (**b**) axial ratio AR; (**c**) antenna gain.

4. Rectenna, the Integration of Rectifier and Antenna

The rectenna is fabricated on FR4 substrate with thickness h = 0.8 mm and dielectric constant $\varepsilon_r = 4.4$ by using the print broad making equipment (MITS; FP-21T model 40).

To accurately model the rectenna simulation characteristics, the Thevenin equivalent circuit, which is represented by input impedance matrix of the antenna $[Z_A]$, is used to simulate the presence of the antenna in the ADS simulation. The impedance matrix is exported from the HFSS EM simulator software. The rectenna characteristics are defined using the Friis equation to determine the received RF power. The measurement setup (shown in Figure 7) is done as follows: a CP antenna (same as used for the rectenna fabrication) connected to a function generator is used as the RF transmitter, and the signal source generator power is set to 22 dBm.
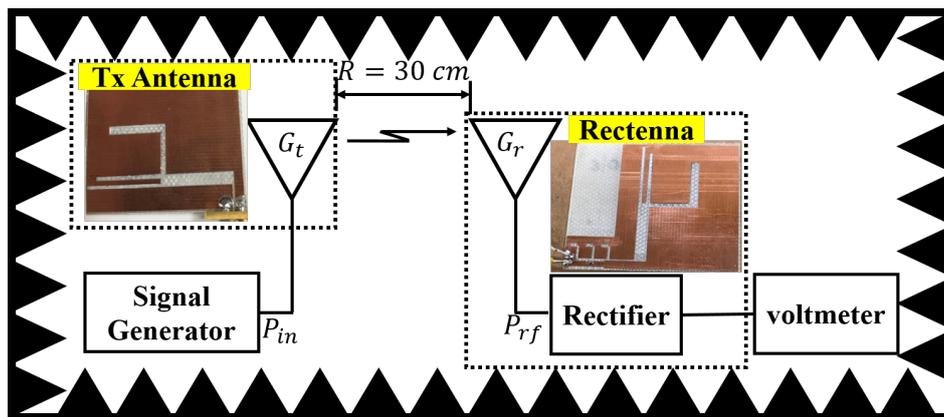
Figure 7. Rectenna measurement setup and the prototype of both the rectenna and antenna are embedded in the figure.

The received RF power P_{rf} is calculated using Friis equation [23]. A suitable definition of the RF-DC conversion efficiency is the ratio of the amount of DC power at the load to the RF input power collected by the antenna, and is given by

$$\eta = \frac{P_{dc}}{P_{rf}} = \frac{V_{dc}}{R_L{}^2 \times P_{rf}} \times 100\%. \tag{1}$$

5. Results and Discussion

The above efficiency includes the antenna efficiency, mismatch, coupling from antenna to the rectifier and rectification efficiencies. The rectenna output performance is estimated using Equation (1) and the efficiency for different constraints is plotted in Figure 8. From the data shown, it is obvious that the results obtained for measurement, EM and circuit model typically agree over the desired band with maximum efficiency at frequency = 2.4 GHz. The variation of conversion efficiency with frequency is shown in Figure 8a. The efficiency is still more than 45% over the band of interest and a slight reduction from the simulation results. The slight reduction of the measured efficiency for the higher frequencies inside the operating band is due to the resultant mismatching in the rectifier circuit. The effect of the terminal load is explained in Figure 8b. The peak measured and simulated conversion efficiency are achieved at $R_L = 1.3$ kΩ.

A comparison between the current design and the relevant work is explained in Table 1. The comparison reveals the significant merits of the current study in terms of low power, high efficiency, and compact size features of the proposed design. For instance, the current design is 60%, 47%, and 85.5% smaller than the topologies given in Ref. [12–14], respectively. The most important thing should be noticed is the high-efficiency improvements at power levels less than 0 dBm.

(a)   (b)
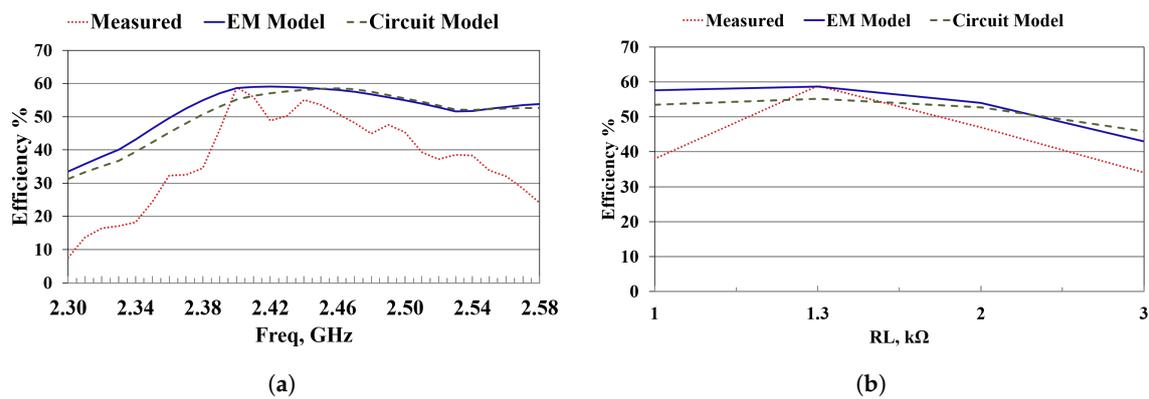
Figure 8. Rectenna simulation and measurement performance characteristics (**a**) efficiency versus frequency at a fixed measured input power −6 dBm, simulated input power −4.5 dBm and $R_L = 1.3$ kΩ; (**b**) efficiency versus terminal load at defined measured input power −6 dBm, simulated input power −4.5 dBm and frequency 2.4 GHz.

Table 1. Comparison of this study with the relevant research work in literature.

Ref.	f, GHz	P_{rf}, dBm	η, %	Polarization	Size, mm³	Sub.
[16]	2.45	≅ −1.5	37.8%	LHCP	60 × 60 × 1.6	FR4
[17]	2.45	−15	28%	HP	49 × 54 × 0.37	Paper
[18]	2.45	22	82.3%	RHCP and LHCP	100 × 100 × 3.8	FR4
This work	2.45	−6	59.5%	LHCP	41 × 35.5 × 0.8	FR4

6. Conclusions and Future Work

This letter has explained a new method to design compact, circular-polarized, highly efficient rectenna that can work at low input power less than 0 dBm, typically −6 dBm. A high-efficiency 2.45 GHz rectenna with simple structure, low-cost fabrication, and the single-feed network has been proposed and investigated. The configuration of the proposed antenna design is very simple and provides high flexibility in the operating frequency of the antenna design and fabrication. It is demonstrated that the overall efficiency of the proposed rectenna can achieve 59.5% with RF input power of −6 dBm. Since the RF-to-DC conversion efficiency has evolved as an important research topic for low-power RF energy harvesting, this work can be considered as a successful attempt in this respect. Future improvement will include the deployment of antenna array elements. Several distributed arrays of antennas, which are designed by scaling in array size, power, DC load, frequency, and gain level, are presented to increase harvested power and efficiency.

Conflicts of Interest: The authors declare no conflict of interest.

References

1. Finkenzeller, K. *RFID Handbook—Fundamentals and Applications in Contactless Smart Cards and Identification*; Wiley: West Sussex, UK, 2003; pp. 41–53.
2. Dobkin, D.M. *The RF in RFID: Passive UHF RFID in Practice*; Newnes: Newton, MA, USA, 2007; pp. 19–34.
3. Popović, Z. Cut the cord: Low-power far-field wireless powering. *IEEE Microw. Mag.* **2013**, *14*, 55–62. [CrossRef]
4. Mansour, M.M.; Kanaya, H. Compact RF rectifier circuit for ambient energy harvesting. In Proceedings of the IEEE International Symposium on Radio-Frequency Integration Technology (RFIT), Seoul, Korea, 30 August–1 September 2017; pp. 220–222.
5. Mansour, M.M.; Kanaya, H. Compact and Broadband RF Rectifier With 1.5 Octave Bandwidth Based on a Simple Pair of L-Section Matching Network. *IEEE Microw. Wirel. Compon. Lett.* **2018**, *28*, 335–337. [CrossRef]
6. Mansour, M.M.; Kanaya, H. Efficiency-Enhancement of 2.45-GHz Energy Harvesting Circuit Using Integrated CPW—MS Structure at Low RF Input Power. *IEICE Trans. Electron.* **2019**, *E102-C*, 399–407. [CrossRef]
7. Mansour, M.; Le Polozec, X.; Kanaya, H. Enhanced Broadband RF Differential Rectifier Integrated with Archimedean Spiral Antenna for Wireless Energy Harvesting Applications. *Sensors* **2019**, *19*, 655. [CrossRef] [PubMed]
8. Mansour, M.M.; Kanaya, H. High-Efficient Broadband CPW RF Rectifier for Wireless Energy Harvesting. *IEEE Microw. Wirel. Compon. Lett.* **2019**, *29*, 288–290. [CrossRef]
9. Suh, Y.H.; Chang, K. A high-efficiency dual-frequency rectenna for 2.45- and 5.8-GHz wireless power transmission. *IEEE Trans. Microw. Theory Tech.* **2002**, *50*, 1784–1789. [CrossRef]
10. Marian, V.; Allard, B.; Vollaire, C.; Verdier, J. Strategy for microwave energy harvesting from ambient field or a feeding source. *IEEE Trans. Power Electron.* **2012**, *27*, 4481–4491. [CrossRef]
11. Takhedmit, H.; Cirio, L.; Costa, F.; Picon, O. Transparent rectenna and rectenna array for RF energy harvesting at 2.45 GHz. In Proceedings of the 8th European Conference on Antennas and Propagation (EuCAP 2014), Hague, The Netherlands, 6–11 April 2014; pp. 2970–2972.
12. Assimonis, S.D.; Bletsas, A. Energy harvesting with a low-cost and high efficiency rectenna for low-power input. In Proceedings of the IEEE Radio and Wireless Symposium (RWS), Newport Beach, CA, USA, 19–23 January 2014; pp. 229–231.
13. Vyas, R.; Nishimoto, H.; Tentzeris, M.; Kawahara, Y.; Asami, T. A battery-less, energy harvesting device for long range scavenging of wireless power from terrestrial tv broadcasts. In Proceedings of the IEEE/MTT-S International Microwave Symposium Digest, Montreal, QC, Canada, 17–22 June 2012; pp. 1–3.
14. Pinuela, M.; Mitcheson, P.D.; Lucyszyn, S. Ambient RF energy harvesting in urban and semi-urban environments. *IEEE Trans. Microw. Theory Tech.* **2013**, *61*, 2715–2726. [CrossRef]
15. Ren, Y.-J.; Chang, K. 5.8-GHz circularly polarized dual-diode rectenna and rectenna array for microwave power transmission. *IEEE Trans. Microw. Theory Tech.* **2006**, *54*, 1495–1502.
16. Huang, F.J.; Yo, T.C.; Lee, C.M.; Luo, C.H. Design of circular polarization antenna with harmonic suppression for rectenna application. *IEEE Antennas Wirel. Propag. Lett.* **2012**, *11*, 592–595, . [CrossRef]
17. Palazzi, V.; Kialalakis, C.; Alimenti, F.; Mezzanotte, P.; Roselli, L.; Collado, A.; Georgiadis, A. Design of a ultra-compact low-power rectenna in paper substrate for energy harvesting in the Wi-Fi band. In Proceedings of the IEEE Wireless Power Transfer Conference (WPTC), Aveiro, Portugal, 5–6 May 2016; pp. 1–4.
18. Chou, J.H.; Lin, D.B.; Weng, K.L.; Li, H.J. All Polarization Receiving Rectenna With Harmonic Rejection Property for Wireless Power Transmission. *IEEE Trans. Antennas Propag.* **2014**, *62*, 5242–5249. [CrossRef]

19. Hemour, S.; Zhao, Y.; Lorenz, C.H.P.; Houssameddine, D.; Gui, Y.; Hu, C.M.; Wu, K. Towards Low-Power High-Efficiency RF and Microwave Energy Harvesting. *IEEE Trans. Microw. Theory Tech.* **2014**, *62*, 965–976. [CrossRef]

20. SKYWORKS. Available online: http://www.skyworksinc.com/Product/512/SMS7630-061 (accessed on 1 March 2019).

21. Garg, R.; Bahl, I.; Bozzi, M. *Microstrip Lines and Slotlines*, 3rd ed.; Artech House: London, UK, 2013.

22. Kanaya, H.; Tsukamoto, S.; Hirabaru, T.; Kanemoto, D.; Pokharel, R.K.; Yoshida, K. Energy harvesting circuit on a one-sided directional flexible antenna. *IEEE Microw. Wirel. Compon. Lett.* **2013**, *23*, 164–166. [CrossRef]

23. Balanis, C.A. *Antenna Theory Analysis and Design*, 3rd ed.; John & Wiley Sons: Hoboken, NJ, USA, 2005.